ISSN 1070-3284, Russian Journal of Coordination Chemistry, 2022, Vol. 48, No. 12, pp. 799–807. © Pleiades Publishing, Ltd., 2022.
Russian Text © The Author(s), 2022, published in Koordinatsionnaya Khimiya, 2022, Vol. 48, No. 12, pp. 730–738.

Spin State of Iron(II) Clathrochelate in the Cocrystallization Products with 2-Aminopyridine and 2-Hydroxypyridine

G. L. Denisov[a], A. S. Belov[a], E. G. Lebed'[a], and Yu. V. Nelyubina[a, *]

[a] *Nesmeyanov Institute of Organoelement Compounds, Russian Academy of Sciences, Moscow, Russia*

**e-mail: unelya@ineos.ac.ru*

Received April 29, 2022; revised May 18, 2022; accepted May 19, 2022

Abstract—The cocrystallization of the earlier described carboxy-containing iron(II) clathrochelate (**I**) with 2-hydroxypyridine and 2-aminopyridine affords two new crystalline products: the salt and cocrystal of this complex, respectively, formed by the acid–pyridine two-point heterosynthone, which is often met in multicomponent crystals of aromatic acids and *ortho*-substituted pyridines. The neutral nature of the cocrystallization product with 2-hydroxypyridine violates the rule of pK_a, which is fulfilled in the case of 2-aminopyridine, because of the equilibrium shift in the crystalline phase toward the keto form of 2-hydroxypyridine: pyridone-2. According to the X-ray diffraction (XRD) data, complex **I** in the salt and cocrystal exists in the low-spin state and undergoes no temperature-induced transition in a temperature range of 100–298 K.

Keywords: clathrochelates, XRD, cocrystallization, spin state, supramolecular synthones, temperature-induced spin transition

DOI: 10.1134/S1070328422700099

INTRODUCTION

Interest in transition metal complexes capable of existing in two spin states (low- and high-spin, LS and HS) is caused by a possibility of the reversible transition between them upon the application of an appropriate external action (e.g., temperature or pressure), which can be controlled by the molecular and supramolecular design methods [1]. A similar spin transition accompanied by a sharp change in the magnetic, optical, and other properties of the corresponding complexes makes it possible to produce from them diverse devices and materials [2, 3], including sensors [4] and units of molecular spintronic devices [5] and "soft" robotics [6].

One of the classes of compounds that experience spin transition under the temperature effect [7, 8] are macrobicyclic cobalt(II) tris(dioximate) cell complexes (clathrochelates [9]) [8, 10, 11], which favorably differ from other classes of coordination compounds by high thermal and chemical stability, simplicity of synthesis, and broad possibilities of chemical modification [9]. Although isostructural (to clathrochelates) iron(II) complexes retain their LS or HS states in solutions and crystals [12–14], we have recently succeeded to provide the existence of one of representatives of this series in different spin states by the insertion of the second component (solvent) into the crystalline lattice [15]. An analogous approach implying the cocrystallization of the (pseudo)octahedral iron(II) complexes with the organic compounds (4,4'-bipyridine and its analogs) resulted in the formation of cocrystals in which the chosen LS complex experienced the temperature-induced spin transition [16].

In this work, we synthesized the earlier described [17, 18] iron(II) clathrochelate (**I**) that exists in the LS state and contains two carboxyl groups in the *meta*-positions of both phenyl rings (Scheme 1), owing to which compound **I** resembles dicarboxylic aromatic acids, for example, phthalic or terephthalic acids. This provides wide possibilities to prepare from it two-component systems due to the formation of supramolecular acid–pyridine synthones [19] with different numbers of hydrogen bonds [20–22].

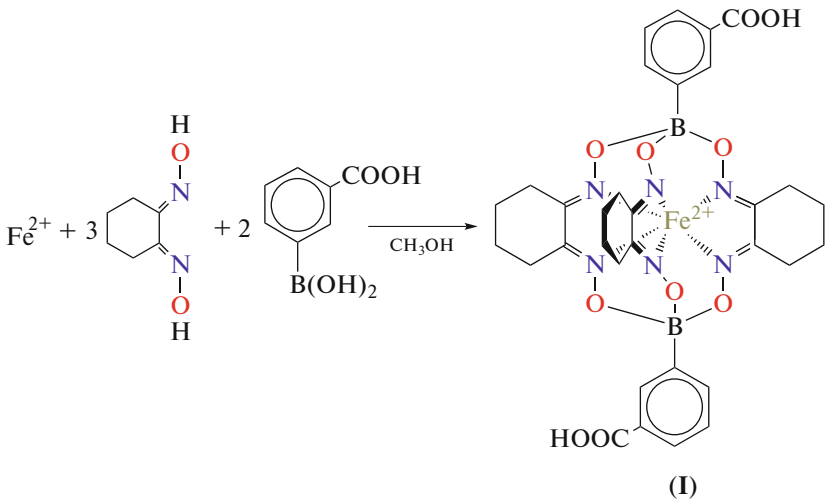

Scheme 1.

2-Hydroxypyridine (2-OH-Py) and 2-aminopyridine (2-NH_2-Py) were chosen as pyridine derivatives for cocrystallization with complex **I**, since they favor the predominant formation of an acid–pyridine synthone compared to the competing acid–acid synthone in cocrystals/salts with carboxylic acids [22]. The acid–acid homosynthone (A) and acid–pyridine one-point (B) and two-point (C) heterosynthones are shown in Scheme 2. The formed crystalline products and the spin state of complex **I** in them were studied by XRD. For one of them, we even succeeded to obtain the XRD data at two different temperatures (100 and 298 K) to draw an unambiguous conclusion about the presence or absence of the temperature-induced spin transition.

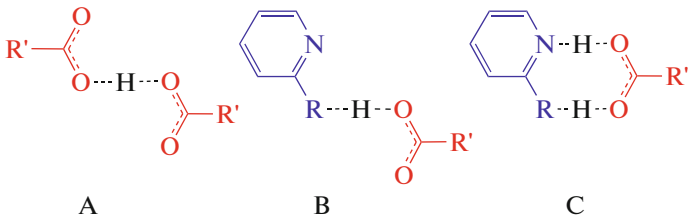

Scheme 2.

EXPERIMENTAL

All procedures were carried out in air using commercially available reagents, organic solvents, and sorbents. Analyses to carbon, nitrogen, and hydrogen were conducted on a Carlo Erba microanalyzer (model 1106). The iron content was determined by spectrophotometry. The ^1H and $^{13}C\{^1H\}$ NMR spectra of a solution of complex **I** in DMSO-d_6 were recorded on a Bruker Avance 600 spectrometer. Chemical shifts were measured relative to the residual signal of this solvent.

Synthesis of $C_{32}H_{34}B_2N_6O_{10}Fe$ (I). Compound $FeCl_2 \cdot 4H_2O$ (0.65 g, 3.26 mmol), nioxime (1.62 g, 11.4 mmol), and *meta*-carboxyphenylboric acid (1.35 g, 8.1 mmol) were dissolved/suspended in methanol (30 mL), and the resulting reaction mixture was stirred at room temperature for 3 h. The formed precipitate was filtered off; washed with methanol (15 mL, 3 portions), diethyl ether (15 mL, 3 portions), and hexane (15 mL, 3 portions); and dried in vacuo with the formation of the target product as an orange finely crystalline powder. The yield was 2.20 g (90%).

^1H NMR (DMSO-d_6; δ, ppm): 1.75 (s, 12H, β-CH_2), 2.85 (s, 12H, α-CH_2), 7.43 (m, 2H, *meta*-Ph), 7.79 (m, 2H, Ph), 7.87 (m, 2H, Ph), 8.18 (s, 2H, Ph), 12.75 (s, 2H, OH). $^{13}C\{^1H\}$ NMR (DMSO-d_6; δ, ppm): 21.25 (s, β-CH_2), 26.34 (s, α-CH_2), 127.81, 129.11, 129.91, 132.97, 136.51 (all s, Ph), 152.78 (s, C=N), 168.46 (s, C=O).

For $C_{32}H_{34}N_6O_{10}B_2Fe$

Anal. calcd., %	C, 51.90	H, 4.59	N, 11.35	Fe, 7.57
Found, %	C, 51.70	H, 4.55	N, 11.22	Fe, 7.70

Cocrystallization of $C_{32}H_{34}B_2FeN_6O_{10}\cdot 2C_5H_5NO\cdot C_2H_3N$ (II). A solution of 2-hydroxypyridine (0.094 g, 0.1 mmol) in acetonitrile (0.3 mL) was added to a solution of complex **I** (0.0374 g, 0.05 mmol) in acetonitrile (1.5 mL). The resulting mixture was heated to the complete dissolution of complex **I** and stored in a closed glass vial at room temperature, which was accompanied by the partial precipitation of an orange powder of complex **I**. The vial was visually inspected at an interval of 3–4 days to monitor the formation of crystalline products for 7 months. After 7 months, several red prismatic crystals of compound **II** formed on the surface of an orange powder of complex **I**.

Cocrystallization of $[C_{32}H_{33}B_2FeN_6O_{10}][C_5H_6N_2]\cdot C_5H_7N_2$ (III). A solution of 2-aminopyridine (0.00188 g, 0.02 mmol) in methanol (0.5 mL) was added to a solution of complex **I** (0.0075 g, 0.01 mmol) in methanol (1.0 mL). The resulting mixture was heated to the complete dissolution of complex **I** and stored in a closed glass vial at room temperature. An orange powder of complex **I** partially precipitated. The vial was visually inspected at an interval of 3–4 days to monitor the formation of crystalline products for 2 months. After 2 months, several red prismatic crystals of salt **III** formed on the surface of an orange powder of complex **I**.

XRD of single crystals of compounds **II** and **III** obtained under the described above cocrystallization conditions was carried out on a Bruker Quest D8 diffractometer (MoK_α radiation, graphite monochromator, ω scan mode) at 100 K. The XRD data at room temperature were additionally obtained for salt **III**. The structures were solved using the ShelXT program [23] and refined by full-matrix least squares using the Olex2 program [24] in the anisotropic approximation for F^2_{hkl}. The hydrogen atoms in the NH and OH groups were localized in the difference Fourier synthesis, positions of other hydrogen atoms were calculated geometrically, and all of them were refined in the isotropic approximation by the riding model. Selected crystallographic data and structure refinement parameters are given in Table 1.

The structural data for compounds **II** and **III** at 100 K and for compound **III** at room temperature were deposited with the Cambridge Crystallographic Data Centre (CIF files CCDC nos. 2168570, 2168571, and 2168572, respectively; http://www.ccdc.cam.ac.uk/).

RESULTS AND DISCUSSION

Iron(II) clathrochelate (**I**) containing carboxyl groups in the apical positions was synthesized using an earlier described procedure [18] by the direct template reaction of nioxime, *meta*-carboxyphenylboric acid, and aqueous iron(II) chloride (Scheme 1). Complex **I** was isolated in the individual form (finely crystalline orange powder) and characterized by elemental analysis and NMR spectroscopy.

Synthesized complex **I** was cocrystallized with two *ortho*-substituted pyridines 2-OH-Py and 2-NH_2-Py in a ratio of 1 : 2 in an appropriate solvent (acetonitrile and methanol, respectively) providing a high solubility of both components. This was accompanied by the partial precipitation of an orange powder of the starting complex **I**, the prolonged storage of which in the mother liquor in closed glass vials at room temperature with the regular (at an interval of 3–4 days) visual inspection resulted in the formation of several red single crystals that were studied by XRD. Unfortunately, a minor amount of the product obtained in both cases did not allow us to apply other popular methods for the characterization of the crystal and electronic structures of the systems based on the iron(II) complexes, including Mössbauer spectroscopy, powder XRD, or NMR spectroscopy of paramagnetic compounds. Attempts to optimize the cocrystallization conditions by using other component ratios (1 : 1 and 2 : 1) or other solvents (DMF, dichloromethane) resulted in the formation of a powder of the starting complex **I**, its single crystals, or single crystals of *ortho*-substituted pyridines.

According to the XRD data, the cocrystallization product of complex **I** with 2-OH-Py was cocrystal **I**$\cdot 2C_5H_5NO\cdot C_2H_3N$ (**II**) with two pyridone-2 molecules corresponding to the preferred tautomeric form of 2-OH-Py in the crystalline phase [25, 26] (Fig. 1a) and one solvate molecule of acetonitrile. On the contrary, its crystallization with 2-NH_2-Py affords salt $[C_5H_7N_2]^+[\mathbf{I}]^-\cdot C_5H_6N_2$ (**III**) due to the proton transfer from one of the carboxyl groups of complex **I** to 2-aminopyridine, which transforms into the cationic form (Fig. 1b). The presence of a neutral molecule of 2-NH_2-Py in the crystal is consistent with the value of ΔpK_a (Table 2) for two components when using benzoic or isophthalic acid as an isostructural analog of complex **I** (Table 2).

In fact, a two-component system of both the neutral and ionic nature can be formed depending on the choice of carboxylic acid and organic base for cocrystallization [27]. According to the pK_a rule [28, 29], the salt is formed at $\Delta pK_a > 3$, and the cocrystal is formed at $\Delta pK_a < -1$. If this value falls onto the intermediate range of ΔpK_a, then the molecular and ionic forms are equally probable, which is observed in the case of salt **III** (Table 2). The formation of cocrystal **II** instead of the predicted salt is due to the existence of 2-OH-Py in the form of *keto*-tautomer [25, 26] preventing the proton transfer from the carboxyl group of complex **I** to the nitrogen atom of pyridine.

Regardless of the nature of the indicated crystalline products, one carboxyl/carboxylate group of complex **I** forms the two-point variant of the classical acid–pyridine supramolecular synthone [19]

Table 1. Selected crystallographic data and structure refinement parameters for cocrystal **II** and salt **III** at 100 K and room temperature (RT)

Parameter	Value		
	II	**III** (100 K)	**III** (RT)
Empirical formula	$C_{44}H_{47}B_2FeN_9O_{12}$	$C_{42}H_{46}B_2FeN_{10}O_{10}$	$C_{42}H_{46}B_2FeN_{10}O_{10}$
Molecular weight	971.37	928.36	928.36
T, K	100	100	298
Crystal system	Triclinic	Monoclinic	Monoclinic
Space group	$P\bar{1}$	$P2_1/c$	$P2_1/c$
Z	2	4	4
a, Å	11.0256(5)	9.3082(2)	9.3939(5)
b, Å	14.1914(6)	18.6468(4)	18.7352(10)
c, Å	14.6082(6)	24.6575(6)	24.7326(13)
α, deg	101.489(2)	90	90
β, deg	90.061(2)	95.9810(10)	95.961(3)
γ, deg	106.841(2)	90	90
V, Å^3	2139.65(16)	4256.46(17)	4329.3(4)
ρ_{calc}, g/cm^{-3}	1.508	1.449	1.424
μ, cm^{-1}	4.30	4.26	4.19
F(000)	1012	1936	50
$2\theta_{max}$, deg	54	54	50
Number of measured reflections	23334	48745	104553
Number of independent reflections	9176	9284	7617
Number of reflections with $I > 3\sigma(I)$	6731	6166	5125
Number of refined parameters	614	624	632
R_1	0.0608	0.0572	0.0451
wR_2	0.1278	0.1493	0.1302
GOOF	1.025	1.028	1.014
Residual electron density (max/min), e Å^{-3}	0.847/–0.694	0.676/–0.409	0.401/–0.313

Table 2. Assumed values of ΔpK_a for the components of cocrystal **II** and salt **III** based on the data for isostructural aromatic acids

Component (pK_a*)	Benzoic acid (3.98)	Isophthalic acid (3.70)	Theory	Experiment
2-OH-Py (12.02)	8.32	8.04	Salt	Cocrystal
2-NH_2-Py (6.67)	2.97	2.69	Possible formation of cocrystal and salt	Cocrystal and salt

* The values of pK_a were taken from the Sci-Finder database.

(Scheme 2), which is met in the two-component systems of carboxylic acids with different pyridines [22, 27, 30], and the second group is bound only to the *ortho*-substituent of the neutral molecule of pyridone-2 or 2-NH_2-Py (Fig. 1). In both cases, the *ortho*-substituent in the chosen pyridine acts as either a hydrogen bond donor as in salt **III** (N...O 2.812(4) and 2.906(4) Å, NHO 167.5(2)° and 153.9(2)° at 100 K), or a hydrogen bond acceptor as in cocrystal **II** (O...O 2.568(4) and 2.589(3) Å, OHO 161.18(15)° and 166.72(16)°). This hydrogen bond results in N–H...O/O–H...N bond weakening in the two-point acid–pyridine heterosynthone (N...O 2.835(4) and 2.705(4) Å, NHO 167.86(18)° and 174.7(2)° at 100 K for compounds **II** and **III**, respectively) compared to the one-point analog (Scheme 2), for example, in the

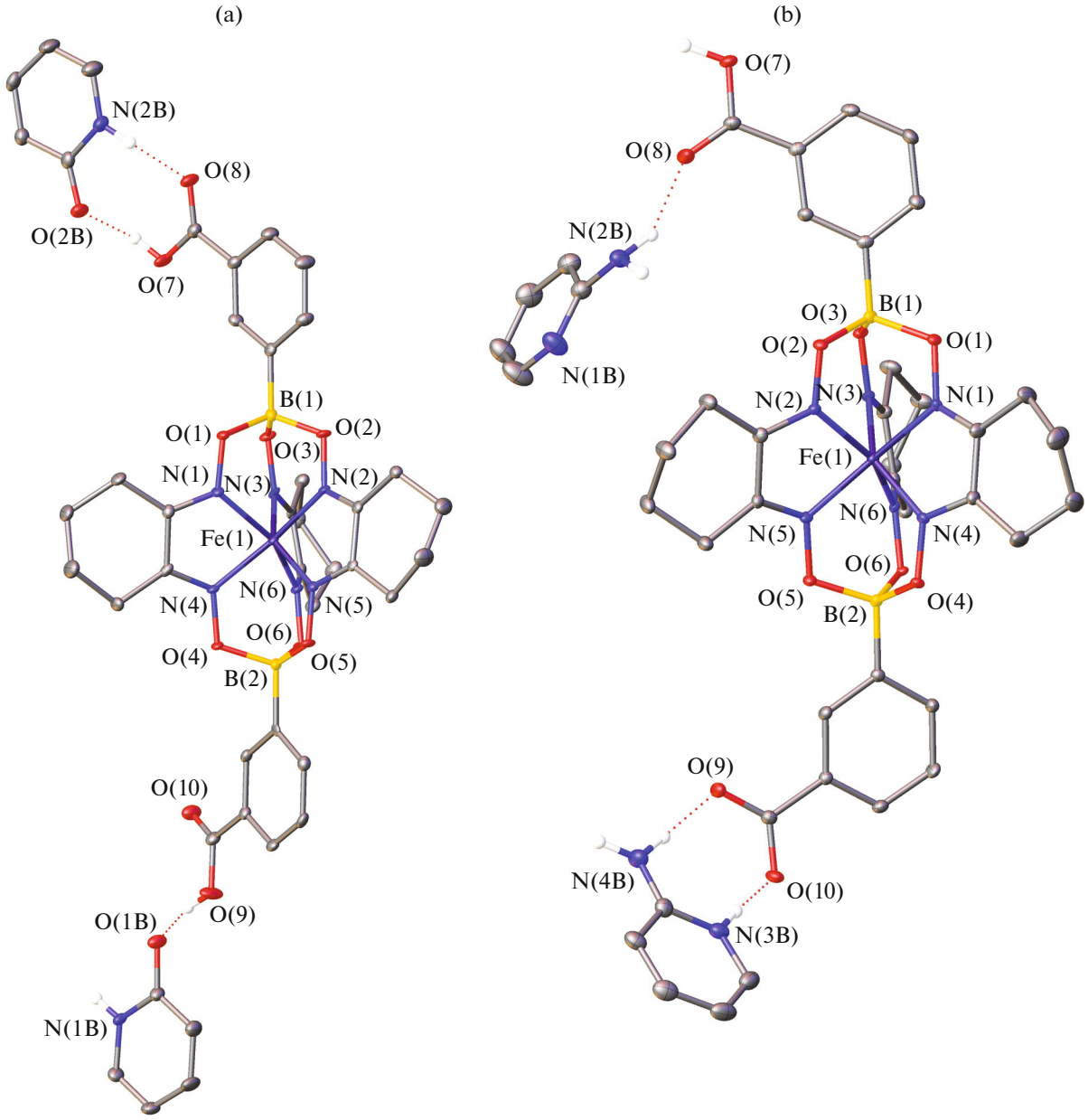

Fig. 1. General view of complex **I** in (a) cocrystal **II** and (b) salt **III** in the representation of atoms by thermal vibration ellipsoids (p = 50%). Hydrogen atoms at the carbon atoms are omitted for clarity, and the solvate acetonitrile molecule in cocrystal **II** and the minor component of the disordered complex anion in salt **III** are also omitted. Numeration is given for heteroatoms only.

series of cocrystals and salts of monobasic aromatic acid with pyridines unsubstituted at the *ortho*-position (N...O 2.653 and 2.575(4) Å, NHO 170.9° and 173.3° on the average, respectively) [22]. However, this bond increases the probability of formation of the acid–pyridine heterosynthone compared to the competing acid–acid homosynthone (Scheme 2) characteristic of mono- and dibasic aromatic acids, for example, benzoic [31], terephthalic, and isophthalic acids [19]. The proton transfer from the carboxyl group of complex **I** to one of the 2-NH_2-Py molecules in crystal of salt **III** favors the formation of both hetero- [20, 21] and homosynthones (Fig. 2). The corresponding hydrogen bonds O–H...O between the carboxylate and carboxyl groups (O...O 2.582(4) Å, OHO 169.66(17)°) join the complex anions into infinite zigzag chains along the crystallographic *b* axis. The second oxygen atom of the carboxylate group, which is not involved in homosynthone formation, is additionally bound to the amino group of the neutral 2-NH_2-Py molecule (N...O 3.152(4) Å, NHO 175.8(2)°).

Cocrystal **II** contains centrosymmetric dimers of pyridone-2 formed by hydrogen bonds N–H...O

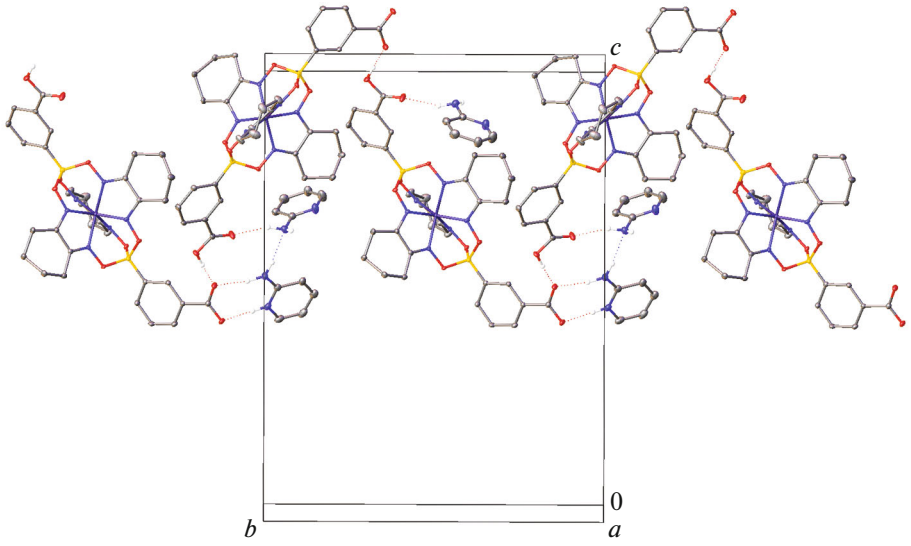

Fig. 2. Fragment of the crystal packing of salt **III** illustrating the formation of hydrogen-bonded zigzag chains of anions of complex **I** along the crystallographic *b* axis. Hydrogen atoms at the carbon atoms, minor component of the disordered complex anion, and cations and neutral molecules of 2-NH_2-Py are omitted.

(N...O 2.771(4) Å, NHO 174.09(19)°) (Fig. 3) instead of the acid–acid homosynthone described above, due to which the main supramolecular motif is an associate composing four 2-O-PyH molecules and two molecules of complex **I** (Fig. 3). These associates are joined with each other via stacking interactions between the pyridone-2 molecules and phenyl groups of the adjacent molecules of complex **I** with the distance between the centroids of the corresponding aromatic rings equal to 3.701(2)–3.9107(18) Å and an angle between them of 160.02(11)°–175.04(11)°. On the contrary, the crystal packing of salt **III** is the three-dimensional hydrogen-bonded cage (Fig. 4) additionally stabilized by hydrogen bonds N–H...N pairwise joining the molecules and cations of 2-NH_2-Py (N...N 3.063(5) Å, NHN 175.8(3)°) (Fig. 2). In addition, these cations form stacking interactions with each other and with the carboxyphenyl groups of the anions (distances between the centroids of the aromatic rings and angles between them are 3.756(2)–3.977(3) Å and 0.00(3)°–9.91(12)°, respectively).

In spite of different natures of the cocrystallization product of complex **I** with the chosen *ortho*-substituted pyridines and different combinations of the formed homo- and heterosynthones, the molecular geometries of this complex in cocrystal **II** and salt **III** differ insignificantly (Fig. 5). The main distinction concerns the turn of the carboxyphenyl groups relatively to the ribbed fragments of the cell ligand, whose angle relatively to the nearest fragment is 27.2(3)° and 16.9(4)° on the average. In both cases, the coordination environment of the iron(II) ion in complex **I** is close to a trigonal prism (TP), including at room temperature (Fig. 1). For instance, the distortion angle φ equal to 0° for an ideal TP and 60° for an ideal trigonal antiprism (TAP) is about 19° in compounds **II** and **III**, which slightly differs from an analogous value (Table 3) for the earlier described [32] solvate of complex **I** with DMSO. The coordination polyhedron is characterized more precisely by the so-called "symmetry measures" [33] that describe its deviation from an ideal polyhedron. The lower these values, the better the description of the coordination polyhedron by the corresponding polyhedron. In cocrystal **II** and salt **III**, as in the solvate of complex **I** with DMSO [32], the minimum symmetry measures estimated from the XRD data using the Shape 2.1 program correspond to TP (Table 3).

Although a trigonal prismatic distortion of the (pseudo)octahedral environment of the metal ion is characteristic of the iron(II) complexes in the HS state [1], the Fe–N bond lengths of complex **I** in cocrystal **II** and salt **III** correspond to the values expected to the LS state of the iron(II) ion [1] even at room temperature (Table 3). The absence of a temperature-induced spin transition to the HS state in these crystalline products is also indicated by the red color of their crystals, which was retained on cooling/heating in a temperature range of 100–298 K. A similar situation was observed previously [32] for the crystalline solvate of complex **I** and DMSO (Table 3), whose molecules formed hydrogen bonds with both carboxyl groups (O...O 2.588(6) Å, OHO 169.8(3)°), because of which no expected acid–acid supramolecular homosynthones were obtained. The TP form of the coordination polyhedron of the iron(II) ion in the listed crystalline products is due to the rigidity of the cell ligand preventing turning its ribbed fragments toward the TAP geometry, which stabilizes the HS state of the iron(II) clathrochelates [15].

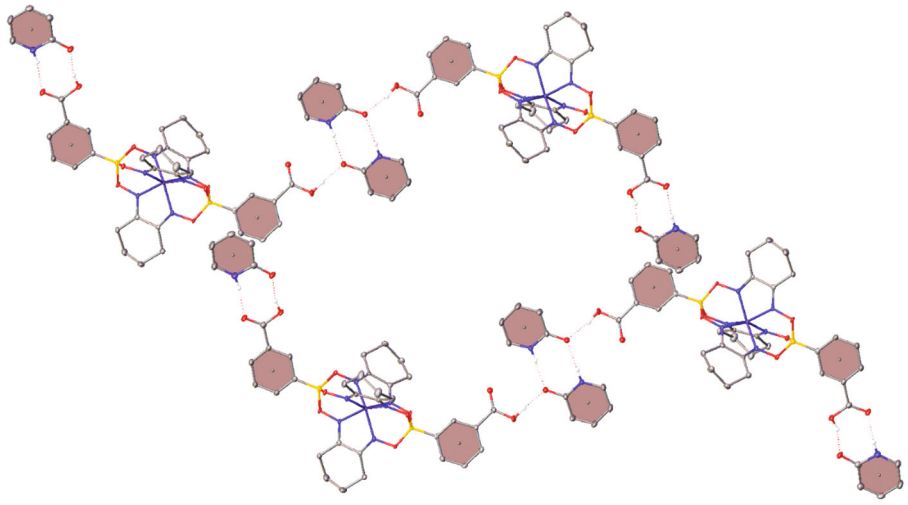

Fig. 3. Fragment of the crystal packing of cocrystal **II** illustrating the formation by pyridone-2 molecules of centrosymmetric hydrogen-bonded dimers and stacking interactions with the phenyl groups of complex **I** (shown by pink) bound to each other via stacking interactions. Hydrogen atoms at the carbon atoms and solvate acetonitrile molecules are omitted.

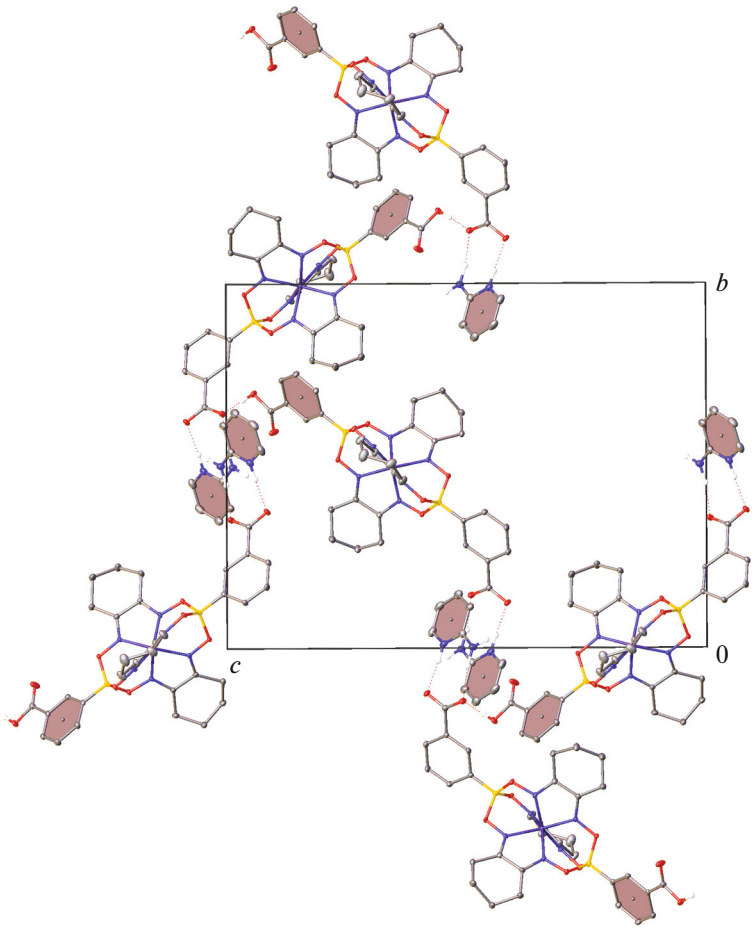

Fig. 4. Fragment of the crystal packing of salt **III** illustrating the formation of stacking interactions between the aromatic fragments of the complex anion and pyridinium cations (shown by pink). Hydrogen atoms at the carbon atoms, minor component of the disordered complex anion, and pyridine molecules are omitted.

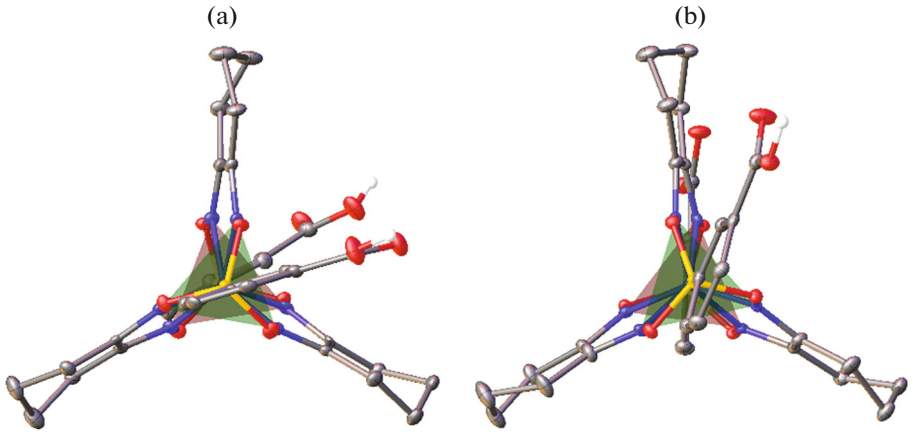

Fig. 5. General view of complex **I** in (a) cocrystal **II** and (b) salt **III** at 100 K along the normal to the planes formed by two sets of the nitrogen atoms of the cell ligand (colored by pink and green). Hydrogen atoms at the carbon atoms and the minor component of the disordered complex anion in salt **III** are omitted.

Table 3. Selected geometric parameters* for complex **I** in cocrystal **II**, salt **III****, and previously described [32] crystalline solvate **I**·$(DMSO)_2$

Parameter	Value			
	II	**III** (100 K)	**III** (RT)	**I**·$(DMSO)_2$
Fe–N, Å	1.886(4)–1.924(4)	1.886(4)–1.924(4)	1.884(4)–1.932(4)	1.908(4)–1.916(4)
φ, deg	19.44(17)	19.6(2)	18.8(2)	21.94(3)
h, Å	2.3542(18)	2.355(3)	2.359(3)	2.349(5)
S(TP)	1.982	2.050	1.957	2.554
S(TAP)	7.959	7.815	7.996	6.924

* φ is the TP-TAP distortion angle of the coordination polyhedron of the iron(II) ion, *h* is the height of this polyhedron, and S(TP) and S(TAP) are deviations of the FeN_6 polyhedron from an ideal trigonal prism (TP) and an ideal trigonal antiprism (TAP), respectively.
** The values are given for the major component of the disordered complex anion in crystal of salt **III** at 100 K and RT.

Thus, the cocrystallization of the earlier described carboxy-containing iron(II) clathrochelate with two *ortho*-substituted pyridines gave new two-component crystals of this clathrochelate of the neutral and ionic nature: the cocrystal with 2-hydroxypyridine in the form of its preferred isomer pyridone-2 and 2-aminopyridine salt. According to the XRD results (primarily to the Fe–N bond lengths), the iron(II) ion of this complex retains its LS state and undergoes no spin transition in the temperature range from 100 K to room temperature. The neutral nature of the cocrystallization product with 2-hydroxypyridine violates the pK_a rule, which is caused by the existence of the latter in the form of pyridone-2 being its preferred tautomer in the crystalline phase, whereas for the salt with pyridone-2 the formation of simultaneously molecular and ionic associates is observed in full correspondence with the pK_a rule. In spite of these distinctions, the supramolecular organization of the salt and cocrystal is based on the acid–pyridine two-point heterosynthone, which is frequently met in multicomponent crystals of aromatic acids and *ortho*-substituted pyridines.

ACKNOWLEDGMENTS

Elemental analysis was supported by the Ministry of Science and Higher Education of the Russian Federation using the scientific equipment of the Center of Investigation of Structure of Molecules at the Nesmeyanov Institute of Organoelement Compounds (Russian Academy of Sciences).

FUNDING

This work was supported by the Russian Science Foundation, project no. 19-73-10194.

CONFLICT OF INTEREST

The authors declare that they have no conflicts of interest.

REFERENCES

1. *Spin Crossover Materials: Properties and Applications*, Halcrow, M.A., Ed., Chichester: Wiley, 2013.
2. Molnár, G., Rat, S., Salmon, L., et al., *Adv. Mater.*, 2017, vol. 30, no. 5, p. 1703862.
3. Senthil Kumar, K. and Ruben, M., *Coord. Chem. Rev.*, 2017, vol. 346, p. 176.
4. Linares, J., Codjovi, E., and Garcia, Y., *Sensors*, 2012, vol. 12, p. 4479.
5. Coronado, E., *Nature Rev. Mat.*, 2020, vol. 5, no. 2, p. 87.
6. Enriquez-Cabrera, A., Rapakousiou, A., Piedrahita Bello, M., et al., *Coord. Chem. Rev.*, 2020, vol. 419, p. 213396.
7. Voloshin, Y.Z., Varzatskii, O.A., Novikov, V.V., et al., *Eur. J. Inorg. Chem.*, 2010, vol. 2010, no. 34, p. 5401.
8. Novikov, V.V., Ananyev, I.V., Pavlov, A.A., et al., *J. Phys. Chem. Lett.*, 2014, vol. 5, no. 3, p. 496.
9. Voloshin, Y., Belaya, I., and Krämer, R., *Cage Metal Complexes: Clathrochelates Revisited*, Springer, 2017.
10. Vologzhanina, A.V., Belov, A.S., Novikov, V.V., et al., *Inorg. Chem.*, 2015, vol. 54, no. 12, p. 5827.
11. Dolganov, A.V., Belov, A.S., Novikov, V.V., et al., *Dalton Trans.*, 2015, vol. 44, no. 5, p. 2476.
12. Pavlov, A.A., Savkina, S.A., Belov, A.S., et al., *Inorg. Chem.*, 2017, vol. 56, no. 12, p. 6943.
13. Voloshin, Y.Z. Varzatskii, O.A., et al., *Inorg. Chem.*, 2000, vol. 39, no. 9, p. 1907.
14. Varzatskii, O.A., Penkova, L.V., Kats, S.V., et al., *Inorg. Chem.*, 2014, vol. 53, no. 6, p. 3062.
15. Denisov, G.L., Novikov, V.V., Belova, S.A., et al., *Cryst. Growth Des.*, 2021, vol. 21, no. 8, p. 4594.
16. Birchall, L.T., Truccolo, G., Jackson, L., and Shepherd, H.J., *Chem. Sci.*, 2022, vol. 13, no. 11, p. 3176.
17. Marmier, M., Wise, M.D., Holstein, J.J., et al., *Inorg. Chem.*, 2016, vol. 55, no. 8, p. 4006.
18. Lebed, E.G., Belov, A.S., Dolganov, A.V., et al., *Inorg. Chem. Commun.*, 2013, vol. 30, p. 53.
19. Bis, J.A. and Zaworotko, M.J., *Cryst. Growth Des.*, 2005, vol. 5, no. 3, p. 1169.
20. Vishweshwar, P., Nangia, A., and Lynch, V.M., *Org. Chem.*, 2002, vol. 67, no. 2, p. 556.
21. Mukherjee, A. and Desiraju, G.R., *Cryst. Growth Des.*, 2014, vol. 14, no. 3, p. 1375.
22. Denisov, G.L. and Nelyubina, Y.V., *Crystals*, 2022, vol. 12, no. 4, p. 497.
23. Sheldrick, G.M., *Acta Crystallogr., Sect. A: Found. Crystallogr.*, 2008, vol. 64, p. 112.
24. Dolomanov, O.V., Bourhis, L.J., Gildea, R.J., et al., *J. Appl. Crystallogr.*, 2009, vol. 42, p. 339.
25. Yang, H.W. and Craven, B.M., *Acta Crystallogr., Sect. B: Struct. Sci.*, 1998, vol. 54, p. 912.
26. De Kowalewski, D.G., Contreras, R.H., Diez, E., and Esteban, A., *Mol. Phys.*, 2004, vol. 102, no. 23, p. 2607.
27. Mohamed, S., Tocher, D.A., Vickers, M., et al., *Cryst. Growth Des.*, 2009, vol. 9, no. 6, p. 2881.
28. Cruz-Cabeza, A.J., *CrystEngComm*, 2012, vol. 14, no. 20, p. 6362.
29. Lemmerer, A., Govindraju, S., Johnston, M., et al., *CrystEngComm*, 2015, vol. 17, no. 19, p. 3591.
30. Sarma, B., Nath, N.K., Bhogala, B.R., and Nangia, A., *Cryst. Growth Des.*, 2009, vol. 9, no. 3, p. 1546.
31. Moragues-Bartolome, A.M., Jones, W., and Cruz-Cabeza, A.J., *CrystEngComm*, 2012, vol. 14, no. 7, p. 2552.
32. Marmier, M., Wise, M.D., Holstein, J.J., et al., *Inorg. Chem.*, 2016, vol. 55, no. 8, p. 4006.
33. Alvarez, S., *Chem. Rev.*, 2015, vol. 115, p. 13447.

Translated by E. Yablonskaya